1   **IL-15 re-programming compensates for NK cell mitochondrial dysfunction in HIV-1 infection**
2

3   Elia Moreno Cubero[1], Stefan Balint[2], Aljawharah Alrubayyi[1], Ane Ogbe[1], Rebecca Matthews[3], Fiona
4   Burns[3,4], Sarah Rowland-Jones[1], Persephone Borrow[1], Anna Schurich[5], Michael Dustin[2], Dimitra
5   Peppa[1,6*]
6   [1]Nuffield Dept of Clinical Medicine, University of Oxford, UK, [2]Kennedy Institute of Rheumatology,
7   University of Oxford, [3]Institute for Global Health UCL, London, UK, [4]Royal Free London NHS Foundation
8   Trust, London, United Kingdom, [5]School of Immunology and Microbial Sciences, King's College
9   London, [6]Mortimer Market Centre, Department of HIV, CNWL NHS Trust, London, UK.
10

11   *Correspondence:*
12   Dimitra Peppa
13   dimitra.peppa@ndm.ox.ac.uk

14   Keywords: Natural Killer cells, HIV-1, IL-15, metabolism, HCMV
15
16   **Abstract**

17   Dynamic regulation of cellular metabolism is important for maintaining homeostasis and can directly
18   influence immune cell function and differentiation including Natural Killer (NK) cell responses.
19   Persistent HIV-1 infection leads to a state of chronic activation, subset redistribution and progressive
20   NK cell dysregulation. In this study we examined the metabolic processes that characterise NK cell
21   subsets in HIV-1 infection, including adaptive NK cell subpopulations expressing the activating
22   receptor NKG2C, which expand during chronic infection. These adaptive NK cells exhibit an enhanced
23   metabolic profile in human cytomegalovirus (HCMV) infected HIV-1 seronegative individuals.
24   However, the bioenergetic advantage of adaptive CD57+NKG2C+ NK cells is diminished during chronic
25   HIV-1 infection, where NK cells uniformly display reduced oxidative phosphorylation (OXPHOS) and
26   limited fuel flexibility upon CD16 stimulation. Defective OXPHOS was accompanied by increased
27   mitochondrial depolarisation and structural alterations indicative of mitochondrial dysfunction,
28   suggesting that mitochondrial defects are restricting the metabolic plasticity of NK cell subsets in HIV-
29   1 infection. The metabolic requirement for receptor stimulation was alleviated upon IL-15 pre-
30   treatment enhancing mammalian target of rapamycin complex1 (mTORC1) activity and NK cell
31   functionality in HIV-1 infection, representing an effective strategy for pharmacologically boosting NK
32   cell responses.
33
34   **Introduction**
35   Natural Killer (NK) cells play a key role in antiviral immunity and a number of studies implicate NK cells
36   as critical contributors to immune control of HIV-1 (Fauci et al., 2005) (Martin et al., 2002) (Martin et
37   al., 2007). It is well documented that persistent HIV-1 infection alters the subset distribution and
38   functional capacity of NK cells (Peppa et al., 2018) (Bradley et al., 2018) (Altfeld et al., 2011). In
39   particular HCMV co-infection, a hallmark of HIV-1 infected cohorts, triggers a dramatic expansion of
40   differentiated NK cells expressing the activating receptor NKG2C, which prototypically characterises
41   adaptive NK cells (Guma et al., 2006) (Mela and Goodier, 2007) (Brunetta et al., 2010). These
42   expanded NKG2C+ NK cells co-express CD57, a marker of maturation, and are influenced by HLA-E
43   presented peptides (Hammer et al., 2018) (Rolle et al., 2018). Notably they resemble memory CD8 T
44   cells and are imbued with enhanced capacity for antibody dependent cellular cytotoxicity (ADCC), in
45   particular increased IFN-γ production attributed to epigenetic remodelling of the IFNG locus (Schlums
46   et al., 2015) (Lee et al., 2015). The adaptive reconfiguration of NK cells during HIV-1 infection is further
47   delineated by loss of the transcription factor promyelocytic leukaemia zinc finger protein (PLZF), and
48   downstream signalling molecules such as FcεRI-γ (Peppa et al., 2018), which partly overlap with
49   NKG2C expression. While these attributes are considered important in the functional specialisation of

50   these NK cells, the development of these features under conditions of continuous
51   stimulation/persistent inflammation during HIV-1 infection could lead to the establishment of
52   functionally and metabolically exhausted NK cells akin to exhausted CD8 T cells. In keeping with this
53   notion, chronic stimulation of adaptive NK cells through NKG2C ligation was recently found to lead to
54   a molecular programme of exhaustion that is shared between NK cells and CD8 T cells (Merino et al.,
55   2019). Exhausted CD8 T cells are characterised by a number of metabolic defects, however, to date it
56   remains unexplored how persistent HIV-1 infection contributes to the metabolic remodelling of NK
57   cell subsets. NK cell exhaustion could influence responses to CD16 engagement linked to vaccine-
58   induced protective immunity against HIV-1 infection and phenotypes of viral control (Scully and Alter,
59   2016). Such knowledge represents a critical first step in our understanding of the metabolic machinery
60   of NK cell subsets with distinct immunologic features that can be potentially targeted for developing
61   new or complementary antiviral approaches aimed at enhancing ADCC responses.

63   Whereas metabolic regulation of T cell function is well characterised, evidence of the importance of
64   immunometabolism in facilitating robust NK cell functions is gradually emerging. Notably, impaired
65   NK cell cellular metabolism has been implicated in obesity and cancer, providing a new framework for
66   understanding NK cell functionality (Michelet et al., 2018) (Cong et al., 2018). Studies from both
67   human and murine models have demonstrated that NK cells activated through cytokine stimulation
68   exhibit substantial increases in the rates of both glycolysis and oxidative phosphorylation (OXPHOS)
69   pathways (Marcais et al., 2014) (Donnelly et al., 2014) (Keating et al., 2016; O'Brien and Finlay, 2019).
70   However, the metabolic requirement of NK cells for optimal effector function, in terms of IFN-γ
71   production, depends on the specific activation stimuli. In particular, receptor mediated activation
72   through anti-NK1.1 and anti-Ly49D in mice appears to require OXPHOS as an essential second signal
73   for IFN-γ production and appears more susceptible to metabolic inhibition compared to cytokine
74   stimulation (Keppel et al., 2015).

76   Different metabolic programmes are adopted by different NK cell subsets and recent evidence
77   suggests that distinct metabolic fingerprints underline the fate of NK cells (Pfeifer et al., 2018; Schafer
78   et al., 2019). Along these lines adaptive NK cells emerging in response to HCMV infection in HIV-1
79   seronegative adults have been reported to engage different metabolic pathways exhibiting enhanced
80   mitochondrial fitness relative to their canonical counterparts (Cichocki et al., 2018). These adaptive
81   CD57+NKG2C+ NK cell subpopulations display superior respiratory capacity supported by increased
82   mitochondrial mass, mitochondrial membrane potential and upregulated genes involved in the
83   electron transport chain (ETC). The enhanced mitochondrial metabolism in adaptive NK cell subsets
84   was found to be regulated by the chromatin-modifying transcriptional regulator AT-rich interactive
85   domain-containing protein 5B (ARID5B) (Cichocki et al., 2018). These features may explain the
86   increased functionality of adaptive NK cell subsets in HCMV seropositive HIV-1 seronegative donors,
87   especially augmented IFN-γ production through CD16 dependent recognition. The latter has been
88   linked to increased activity of the mammalian target of rapamycin complex1 (mTORC1) pathway, a
89   well-established regulator of multiple metabolic processes (Schlums et al., 2015). However,
90   knowledge of NK cell metabolism in other chronic viral infections such as HIV-1, where HCMV
91   coinfection is almost universal and plays a defining role in shaping the NK cell pool, remains in its
92   infancy.

94   In this study we sought to address the metabolic features of NK cell subsets during chronic HIV-
95   1/HCMV co-infection. Our findings show that inefficient OXPHOS and loss of mitochondrial integrity
96   in NK cells during HIV-1 infection influences responses to activating CD16 receptor stimulation. Such
97   defects could be overcome *in vitro* by IL-15 metabolic reprogramming reducing the dependence for
98   receptor-mediated metabolic remodelling.

2

Results

NK cells from treatment naïve viraemic HIV-1 infected patients exhibit reduced oxidative metabolism

To study the metabolic profile of NK cells in HIV-1 infection, accounting for the influence of HCMV co-infection, we isolated NK cells from HCMV seropositive treatment-naïve HIV-1 positive donors and HCMV seropositive HIV-1 negative donors (referred to as controls (CTR)). All donors in this study were HCMV+ and screened for the presence of adaptive CD57+NKG2C+ NK cells (**Fig. S1**) as previously described (Hammer and Romagnani, 2017). An extracellular flux analyser was utilised to analyse their metabolic requirements. The glycolytic rate assay was used to estimate the extracellular acidification rate (ECAR), a measure of lactate production and anaerobic glycolysis at the basal state and after the addition of rotenone and antimycin A, which interfere with complex I and complex III of the electron transport chain (ETC), respectively and 2-deoxy-glucose (2-DG) a competitive inhibitor of glycolysis. Consistent with previous reports baseline activity of NK cells was low in both groups and a non-significant trend towards lower basal ECAR was noted in the HIV infected group (**Fig. 1A, B**). No significant differences in the rates of NK cell glycolysis or glycolytic reserve were detected between the two groups, indicating that there were no major modulations of glycolytic pathways at baseline (**Fig. 1C, D, E**). Next, we assessed mitochondrial respiration by measuring oxygen consumption rates (OCR), a measure of OXPHOS, at basal levels and following the addition of a stressor mix including oligomycin (an ATP synthesis inhibitor), carbonyl cyanide-4 (trifluoromethoxy) phenylhydrazone (FCCP; uncoupling synthesis of ATP from the ETC), and rotenone and antimycin A at the indicated time points (**Fig. 1F**). At rest NK cells utilise preferentially OXPHOS and although no difference in the basal OCR levels was observed in the two groups (**Fig. 1G**) both maximal respiration rate and spare respiratory capacity (SRC) were significantly reduced in NK cells from HIV-1 infected donors (**Fig. 1H, I**) suggestive of altered oxidative metabolism.

Given that adaptive CD56dimCD57+NKG2C+ NK cells are expanded in HIV-1 infection, as a consequence of more frequent HCMV reactivations and ongoing inflammation, representing a large proportion of the peripheral NK cell pool (**Fig. S1**), we sought to determine the relationship between the magnitude of these cells and respiratory capacity. Whereas a positive correlation was observed between the frequencies of adaptive NK cells and maximal respiration in HCMV+ controls (CTR) (**Fig. 1J**) as previously reported (Cichocki et al., 2018), this association was not observed in HIV-1 infected donors, suggesting that the superior metabolic profile of NKG2C+ NK cells is diminished in HIV-1 infection (**Fig. 1J**). Adaptive NK cells are less sensitive to innate cytokines but display augmented responses and in particular higher IFN-γ production through CD16 activation (Schlums et al., 2015). The relationship between the metabolic fitness and effector response in adaptive NK cells upon CD16 triggering in the cohort as a whole is reflected in the correlation between IFN-γ production and maximal respiration (**Fig. 1K**).

OXPHOS is required for NK cell IFN-γ production following CD16 crosslinking

To investigate the requirement of OXPHOS for receptor mediated activation of NK cells we tested the ability of CD56dim NK cells to produce IFN-γ following anti-CD16 stimulation in the presence or absence of oligomycin. Addition of oligomycin significantly impaired NK cell IFN-γ production in response to CD16 triggering in the control group (**Fig. 2A, B**). However, this effect was less prominent in CD56dim and NK cell subsets in HIV-1 infected individuals in keeping with an already suppressed capacity to utilise mitochondrial OXPHOS (**Fig. 2C, Fig. S2A, C, D, F)**). Of note the presence of oligomycin did not affect NK cell survival at the concentration used during the 6 hour stimulation and no decrease in the levels of CD16 expression with oligomycin were observed (data not shown). Glycolytic inhibition by adding the inhibitor 2-DG in the assay abrogated IFN-γ production by NK cells in both study groups (**Fig. 2A-C & Fig. S2A-F**). Inhibition of pyruvate transport into the mitochondria with UK5099 had a more pronounced effect on IFN-γ production by CD56dim and adaptive NK cells in HIV-1 infection as compared to HCMV+ controls (**Fig. 2A, C & Fig. S2D, F**). Inhibition of glutamine, an alternative OXPHOS fuel, with BPTES had a significant effect in reducing IFN-γ from adaptive NK cells

3

152   in HIV-1 infection only (**Fig. S2D,F**). Pre-treatment with etomoxir blocking fatty acid transport into the
153   mitochondria, had no obvious effect on IFN-γ production by CD16 activated NK cells in both the control
154   and HIV-1 infected group, suggesting that fatty acids are not utilised by NK cells under these
155   conditions. (**Fig. 2A-C**) (**Fig. S2A-F**). Together these data suggest that glucose is the primary fuel for
156   OXPHOS required for receptor stimulation by NK cells. However, in contrast to controls, in HIV-1
157   infection NK cells, and especially adaptive subpopulations, are less able to mobilise additional energy
158   resources to power OXPHOS.
159
160   **Adaptive NK cells in HIV-1 infection display evidence of dysfunctional mitochondria**
161   The decrease in SRC in NK cells from HIV-1 positive donors suggested a reduced ability of these cells
162   to produce energy in response to stress or increased work demands and prompted us to further
163   investigate the mitochondrial health of NK cells. In particular, greater SRC is shown to correspond to
164   enhanced mitochondrial fitness, a feature of adaptive NK cells and memory CD8 T cells (Cichocki et
165   al., 2018) (van der Windt et al., 2012). We therefore utilised the ratiometric fluorescent dye JC-1 to
166   assess further the mitochondrial membrane potential (ΔΨm) of NK cells, which represents a key
167   readout of mitochondrial function. NK cells from HIV-1 infected donors displayed a lower ΔΨm
168   especially within adaptive subsets compared to NK cells from HIV-1 seronegative donors (**Fig. 3A,B**).
169   This is exemplified by lower red/green fluorescence intensity ratio of JC1, which does not depend on
170   mitochondrial shape, size or density, suggesting that mitochondrial dysfunction in NK cells, especially
171   of adaptive subpopulations which are enriched in HIV-1 positive donors, constitutes a rate limiting
172   step in their capacity to fuel their energy demands.
173   Mitochondria are dynamic organelles that configure their morphology and number to regulate their
174   function and distribution (Cogliati et al., 2016). To interrogate further the relationship between
175   mitochondrial dysfunction and mitochondrial morphological changes we performed confocal
176   imaging. Isolated NK cells from three HCMV+ HIV-1 seronegative controls and three HIV-1/HCMV
177   seropositive donors with evidence of depolarised mitochondria were stained with MitoTracker Deep
178   Red, that accumulates in active mitochondria and enables localisation. Our results demonstrated that
179   despite no difference in the number of mitochondria (**Fig. 3C, D**), NK cells from HIV-1 infected
180   individuals exhibited mitochondrial structural differences adopting a change in their configuration
181   from a long tubular shape into shrunk small spherical shapes (**Fig. 3C, E, F, G**) and (**S3 and S4 movies**).
182   These data suggest that loss of ΔΨm in NK cells from HIV-1 infected individuals most likely triggers a
183   mitochondrial transformation and collapse of structural support mechanisms (Miyazono et al., 2018).
184   Structural changes in the mitochondria have been related to bioenergetic insufficiency and increased
185   mitochondrial sphericity in T cells in the absence of co-stimulation (Klein Geltink et al., 2017) and could
186   also be a reflection of oxidative damage in the cell (Ahmad et al., 2013). However, analysis of reactive
187   oxygen species (ROS) levels in NK cells from patients with chronic HIV-1 infection compared with those
188   of NK cells from HCMV+ HIV seronegative controls did not show a significant increase in the levels of
189   ROS in HIV-1 infection (data not shown). This could be due to a rescue mechanism, with adaptive NK
190   cells previously described to display elevated levels of BCL-2, which may be important in limiting
191   oxidative stress (Zhang et al., 2013) (Cichocki et al., 2018).
192   The enhanced oxidative metabolism observed in adaptive NK cells from HCMV+ HIV-1 seronegative
193   donors has been reported to depend partly on increased expression of *ARID5B* and induction of genes
194   encoding components of the ETC, including *UQCRB,* the ETC complex III gene (Cichocki et al., 2018).
195   To determine whether there were any differences in the expression of *ARID5B* in isolated NK cells
196   from HCMV+ controls and HIV-1 infected individuals we performed quantitative RT-PCR (qRT-PCR).
197   We confirmed increased levels of *ARID5B* expression in NK cells from HIV-1 infected donors, in keeping
198   with greater expansions of adaptive NK cells in HIV-1 infection, relative to controls (**Fig. S5A**). Our
199   findings therefore suggest that mitochondrial structural disorganisation rather than decreased
200   expression of ARID5B could be potentially affecting the performance of the ETC and metabolic
201   adaptation of NK cells in HIV-1 infection.
202

Treatment with IL-15 compensates for the metabolic defects of NK cells in HIV-1 infection

IL-15 plays a vital role in NK cell survival and differentiation and in priming NK cells for enhanced effector function *in vivo* (Cooper et al., 2002). We therefore investigated whether IL-15 priming *in vitro* could improve NK cell responses to stimulation via CD16 by circumventing the metabolic requirements for efficient receptor mediated activation in HIV-1 seropositive donors. Pre-treatment with IL-15 for 48-72 hours followed by anti-CD16 stimulation led to a striking increase in IFN-γ production by total CD56dim NK cells (**Fig. 4A**) but also canonical and adaptive subsets (**Fig. S6A-D**). Inhibition of OXPHOS with oligomycin in primed NK cells did not affect IFN-γ production in response to receptor stimulation while a small difference in the presence of 2-DG persisted (**Fig. 4A, B**).

IL-15 is known to stimulate multifaceted metabolic activities during maturation of NK cells via the mammalian target of rapamycin complex 1 (mTORC1), a key regulator of cellular metabolism (Marcais et al., 2014). IL-15 signalling and activation of NK cells leads to enhanced glucose uptake and enhanced functionality. Consistent with this IL-15 priming of NK cells from HIV-1 infected donors prior to anti-CD16 stimulation induced greater phosphorylation of the translational regulator S6 kinase (S6), consistent with enhanced mTORC1 signalling in CD56dim NK cells (**Fig. 4C, D**) and subsets (data not shown).

To further evaluate the metabolic effects of IL-15 pre-treatment in the presence or absence of anti-CD16 stimulation in isolated NK cells from HIV-1 infected patients we performed extracellular flux assays to directly analyse metabolic responses. NK cells treated with IL-15 displayed a higher basal ECAR especially in the presence of CD16 coated beads relative to resting NK cells (**Fig. 4E**). No significant increase in the cellular respiratory function as measured by OCR was observed either with IL-15 pre-treatment alone or with CD16 stimulation (**Fig. 4F**). A decreased dependence on OXPHOS was observed in IL-15-treated NK cells especially in the presence of CD16 triggering as evidenced by the decreased ratio of OCR:ECAR compared to basal levels (**Fig. 4G**). These findings indicate that IL-15 increased NK cell metabolism, specifically glycolysis, by-passing the "OXPHOS requirement" for receptor stimulated IFN-γ production.

Discussion

Burgeoning evidence indicates that metabolic plasticity is important for fine tuning immune cell function. Whereas most studies have focused on T cell metabolism during human chronic viral infections, much less is known about the metabolic lifestyle of NK cells in this setting. In this study we assessed for the first time the metabolic profile of NK cell subsets and requirements for production of IFN-γ following receptor stimulation, via CD16 crosslinking, during chronic HIV-1 infection. Our results implicate dysregulated metabolism as an upstream driver of NK cell functional fate. NK cells in viraemic HIV-1 infection are characterised by impaired oxidative phosphorylation, reduced metabolic reserve and mitochondrial defects. IL-15 pre-treatment effectively eliminated the metabolic requisite for receptor stimulation boosting NK cell responses.

In general, resting NK cells are quiescent as evidenced by the low basal levels of glycolysis and OXPHOS. However, NK cells in chronic HIV-1 infection display an inability to rely on mitochondrial function under conditions of increased energy demands as evidenced by the reduction in both maximal respiration and SRC. Although we did not formally test the metabolic profile of adaptive CD57+NKG2C NK cells in this study, due to sample limitations and potential effect of sorting on the redox state of the cells (Llufrio et al., 2018), these cells are enriched and represent a sizeable proportion of the peripheral NK cell pool in HIV-1 infection. Notably, there was no correlation between CD57+NKG2C+ NK cells from HIV-1 infected donors and maximal respiration. This suggests that NK cells in HIV-1 infection do not acquire the characteristic metabolic profile defining HCMV adaptive (CD57+NKG2C+) NK cells in HIV-1 seronegative individuals with NK cell memory-like increased OXPHOS (Cichocki et al., 2018). Alternatively, adaptive subpopulations expressing NKG2C could gradually lose their bioenergetic advantage with progressive HIV-1 infection as a consequence of persistent activation and evolving dysregulation.

5

253 Upon stimulation NK cells configure their metabolic machinery to meet their energy demands and
254 synthesize molecules required for NK cell effector function. Depending on the activating stimulus and
255 length of stimulation NK cells can up-regulate glycolysis and OXPHOS. In this study we focused on
256 receptor stimulation via CD16, a potent activator of NK cell function and an important means of NK
257 cell antiviral control in HIV-1 infection. Global OXPHOS inhibition significantly reduced receptor
258 stimulated NK cell IFN-γ production, which was further attenuated by inhibition of glycolysis in both
259 HIV-1 infected and control individuals, in keeping with glucose being the predominant fuel driving
260 OXPHOS. Similar effects were observed in murine models utilising NK1.1 and Ly49D activating receptor
261 stimulation (Keppel et al., 2015), supporting the notion that OXPHOS is a metabolically required
262 second signal for IFN-γ production mediated via ITAM coupled adapters. Inhibition of alternative fuels,
263 such as glutamine and fatty acids, did not significantly affect IFN-γ production by NK cells in HCMV+
264 control donors, while an effect was observed for NK cell subsets in HIV-1 infection for glutamine and
265 pyruvate suggesting a loss of metabolic plasticity.

266 Metabolic inflexibility has been recently described to underline dysfunctional HIV-specific CD8 T cells
267 (Angin, 2019). In particular, the polyfunctionality of CD8 T cells from spontaneous HIV-1 controllers
268 was more reliant on mitochondrial function rather than glycolysis and differences in glucose
269 dependency described in SIV-specific CD8 T cells have been found to correlate with their capacity to
270 supress SIV infection. We therefore reasoned that the observed inability of NK cells to utilise OXPHOS
271 during HIV-1 infection could reflect dynamic changes in the mitochondria, which are essential hubs of
272 metabolic activity determining the function and fate of immune cells. A global mitochondrial defect
273 was supported by decreased mitochondrial membrane potential (Δψm) in NK cells in HIV-1 infection.
274 Notably, isolated NK cells from HIV-1 infected patients displayed marked changes in mitochondrial
275 architecture characterised by the presence of small spherical mitochondria. The shape of the
276 mitochondria may directly impact their bioenergetic function, with elongated mitochondria being
277 associated with more efficient ATP production, and mitochondrial dysfunction resulting in
278 fragmentation described in a number of pathological conditions (Chan, 2019). Interestingly the
279 delicate balance between mitochondrial fusion and fission controls mitochondrial shape, number and
280 size and is important for function (respiratory capacity) and quality control of mitochondria, raising
281 the possibility that alterations in mitochondrial dynamics in HIV-1 infection could influence NK cell
282 metabolic reprogramming. Along these lines mitochondrial fusion regulated by optic atrophy-1 (OPA-
283 1) was found to facilitate tight cristae organisation in memory T cells (Tm) cells, with continued
284 entrance of pyruvate into mitochondria and efficient ETC activity (Buck et al., 2016). In contrast,
285 effector T cells with fissed mitochondria displayed diffuse internal structures and less efficient
286 OXPHOS, and pharmacological enforcement of mitochondrial fusion promoted oxidative capacity and
287 superior functionality (Buck et al., 2016). It would therefore be important to dissect in future studies
288 the intricate relationship between the modulation of mitochondrial shape and NK cell energetic state
289 and downstream cellular processes, such as mitophagy (O'Sullivan et al., 2015), providing a framework
290 to study these crucial biological interactions on metabolic regulation of NK cell subsets during chronic
291 viral infections.

292 The observed alterations in the metabolic machinery of NK cells during chronic HIV-1 infection
293 influencing their mitochondrial integrity, bears similarities to exhausted CD8 T cells. In particular
294 exhausted CD8 T cells during chronic viral infections show extensive mitochondrial alterations with an
295 impaired ability to use mitochondrial energy supply coupled to the programmed death-1 (PD-1)
296 pathway (Schurich et al., 2016) (Fisicaro et al., 2017) (Bengsch et al., 2016). Signalling via PD-1
297 promoting exhaustion of CD8 T cells has been found not only to affect mitochondrial morphology but
298 also to represses the key metabolic transcriptional regulator peroxisome proliferator-activated
299 receptor-γ (PPAR-γ) coactivator 1a (PGC-1a), controlling energy metabolism and mitochondrial
300 biogenesis, suppressing OXPHOS and glycolysis in virus specific T cells (Bengsch et al., 2016).
301 Upregulation of inhibitory molecules on NK cells could also serve as a pathway supressing their

6

302 metabolic fitness. Recently chronic stimulation of adaptive NKG2C+ NK cells *in vitro* led to a marked
303 induction of checkpoint inhibitory receptors PD-1 and lymphocyte activation gene-3 (LAG-3) sharing
304 epigenetically driven programmes with exhausted CD8 T cells (Merino et al., 2019). Moreover, a role
305 for LAG-3 in regulating CD4 T cell metabolism and mitochondrial biogenesis has been identified
306 (Previte et al., 2019). We have previously reported a modest increase in the levels of PD-1 expression
307 on NK cells in HIV-1 infection (Peppa et al., 2018), however, the role of inhibitory receptors in
308 controlling NK cell metabolism remains to be further defined.

309 Pre-treatment of NK cells with IL-15 alleviated the need for OXPHOS for CD16 receptor stimulated IFN-
310 γ production extending observations from murine models (Keppel et al., 2015). Our results implicate
311 IL-15 increased mTORC1 activity, an important regulator of NK cell metabolism, in upregulating
312 glycolysis. The remaining dependence on glucose could reflect an overall NK cell increased
313 dependency to glycolysis or a switch to a post-transcriptional regulatory mechanism for IFN-γ
314 production as described for T cells (Chang et al., 2013). Notably, the effects of IL-15 priming on NK cell
315 metabolism and functionality have important implications for clinical translation in HIV-1 infection.
316 The beneficial effects of IL-15 immunotherapy and IL-15 superagonist ALT-803, capable of activating
317 both NK cells and CD8 T cells, have been highlighted *in vivo* in non-human primate models (Webb et
318 al., 2018) and such an approach is currently being tested in a phase I clinical trial to facilitate clearance
319 of latent HIV-1 reservoirs (NCT02191098). The ability of IL-15 to enhance ADCC and augment NK cell
320 mediated killing of HIV-infected target cells *ex vivo* (Garrido et al., 2018) may prove vital in the
321 development of a functional cure for HIV. Our findings together with a recent report of IL-15 mediated
322 metabolic reprogramming improving the efficacy of HIV-specific CD8 T cells from non-controllers
323 (Angin, 2019), highlight the complementary effects of such an approach to simultaneously re-
324 invigorate multiple arms of the immune response.

326 In summary, our results demonstrate that NK cells in HIV-1 infection exhibit metabolic defects
327 affecting both canonical and adaptive subsets underlined by mitochondrial dysfunction/structural
328 alterations and bearing similarities to exhausted CD8 T cells described in chronic viral infections. These
329 findings identify mitochondrial centred dysfunction as a key area for future research and as a
330 promising target for future combined reconstitution therapies. IL-15 pre-treatment bypasses the
331 metabolic requirement for OXPHOS upon CD16 mediated activation and potentiates NK cell function,
332 which is of considerable clinical interest in the field of HIV as a powerful multipronged therapeutic
333 strategy. Further insights into the potential role of inhibitory receptors will provide us with a more
334 comprehensive understanding of the integration of signals and the role of metabolism in fine tuning
335 the range and potency of NK cell antiviral functions.

337 **Material and Methods**
338 **Study Subjects**
339 Cryopreserved peripheral blood mononuclear cells (PBMCs) from eleven HIV-1 infected HCMV
340 seropositive treatment naïve patients were utilised (mean age= 38.49, range= 27-49; mean
341 LogVL=4.89, range=4.14-6.33; mean CD4 count 475 cells/mL, range=61-720). Participants were
342 recruited at the Mortimer Market Centre for Sexual Health and HIV Research and the Royal Free
343 Hospital (London, UK) following written informed consent as part of a study approved by the local
344 ethics board committee. Seven demographically age, sex and lifestyle matched HCMV seropositive
345 HIV-1 seronegative donors (mean age=36.9, range=26-49) with sizeable adaptive NK cell responses
346 (>10%) were used for comparison (**Fig. S1**), from whom blood was taken and cryopreserved for later
347 use with written informed consent in accordance with the Declaration of Helsinki. All study
348 participants were anti-Hepatitis C virus antibody negative and anti-HBsAg negative and HCMV
349 seropositive. HCMV serology was determined at University College London Hospital clinical virology
350 lab by the ARCHITECT CMV IgG assay (AU/mL) (Abbott Diagnostics, IL, USA).

351

Flow cytometric analysis

The following fluorochrome-conjugated antibodies were used in this study: CD16 BB700, CD56 BV605, CD57 BV421 (BD Biosciences), CD3 BV650, CD14 BV510, CD19 BV510, CD56 PE Dazzle, CD16 PerCP (BioLegend), NKG2C PE and NKG2C AlexaFluor700 (R&D systems) for surface antigens; IFN-γ PE-CY7, (BD Pharmingen) and pS6 (S235/236) AlexaFluor647 (Cell Signaling) for intracellular antigens. Briefly, cryopreserved PBMC isolated from HIV-1-infected patients and healthy controls were washed in PBS, and surface stained at 4°C for 20 min with saturating concentrations of different combinations of antibodies in the presence of fixable live/dead stain (Invitrogen). Cells were then fixed and permeabilized for detection of intracellular antigens. Assessment of mitochondrial membrane polarisation and ROS production was performed by incubation with 2 μM JC-1 or 5 μM MitoSOX (Invitrogen) respectively according to manufacturer's instructions. Samples were acquired on a BD Fortessa X20 using BD FACSDiva8.0 (BD Bioscience) and data analysed using FlowJo 10 (TreeStar). **Fig. S1** includes the gating strategy for the identification of NK cell subsets into adaptive and canonical on the basis of expression of CD57 and NKG2C.

NK cell isolation

NK cells were enriched from PBMCs using a negative-selection magnetic bead kit (Miltenyi Biotec) as per the manufacturer's instructions (>94% purity and viability).

Extracellular flux assays

Extracellular flux assays were performed using an XFp Analyzer (Agilent technologies). Purified NK cells were seeded at 2×10^5 cells per well in Seahorse cell plates coated with CellTak (Corning). Mitochondrial OXPHOS was evaluated using the mitostress test kit and glycolysis using the glycolytic rate assay kit (Agilent technologies). The oxygen consumption rate (OCR) and extracellular acidification rate (ECAR) were measured in XF RPMI medium supplemented with 10 mM glucose, 1 mM pyruvate and 2 mM glutamine in response to oligomycin (1 μM), FCCP (1 μM), rotenone/antimycin A (0.5 μM) and 2-DG (50 mM) (Agilent technologies). To evaluate the effect on the metabolic profile of IL-15 pre-treatment, NK cells were purified and cultured with 100 ng/mL of IL-15 for 48h, then split and further stimulated with CD16-coated beads (Milteny) or left in IL-15 supplemented media. Maximum respiration is the average OCR values post-FCCP injection. The spare respiratory capacity (SRC) was calculated as average post-FCCP injection minus basal OCR average. Glycolysis was calculated as average basal ECAR values minus post-2-DG injection values. Glycolytic reserve was calculated as average post-rotenone/antimycin A injection ECAR values minus basal ECAR values.

Functional assays

For activation via CD16 cross-linking, 96-well flat-bottom plates (Nunc) were coated with 5 μg/mL anti-human CD16 (clone 3G8, BD Biosciences) or an isotype-matched control antibody (mIgG1κ, BD Biosciences) overnight at 4°C. Plates were washed with sterile PBS before addition of 4×10^5 PBMC per well. To assess fuel flexibility cells were incubated for 6 h in the presence or absence of 100 nM Oligomycin, 50 mM 2-DG, 2 μM UK5099, 3 μM BPTES and 4 μM Etomoxir (Sigma). GolgiStop (containing Monensin, 1/1,500 concentration) (BD Biosciences) and GolgiPlug (containing brefeldin A, 1/1,000 final concentration) (BD Biosciences) were added for the last 5 h of culture. Following incubation cells were washed and stained for extracellular receptors before permeabilization and intracellular staining for IFN-γ and pS6. Where indicated cells were pre-treated with 100 ng/mL IL-15 (Miltenyi) for 48-72h.

Confocal microscopy

Confocal imaging was performed with an Olympus FV1200 inverted microscope (Olympus) equipped with a 60× 1.4 NA oil-immersion objective at room temperature.

8

402 Prior to confocal imaging, purified NK cells were incubated with 50 nM MitoTracker Deep Red FM
403 (ThermoFisher Scientific) for 60 min at 37°C to visualise the mitochondria. After incubation, the cells
404 were plated onto 0.01 % Poly-L-Lysine coated 8-well IBIDI chamber for 15 min followed by fixation
405 with 4% PFA/PBS for additional 30 min at room temperature. An additional labelling with 10 μg/mL
406 WGA-AlexaFluor488 (ThermoFisher Scientific) for 10 min to visualize the cell membrane was
407 performed. Images were taken with a 250 nm z-stepping. Post processing and segmentation (TrakEM2
408 plugin) of fluorescence images was done with ImageJ (National Institute of Health). The number of
409 mitochondria, surface area, mitochondria volume and sphericity were obtained by 3D surface
410 rendering of confocal images in Imaris version 9.3 (Bitplane).
411
412 **Quantification of gene expression**
413 Total NK cells were lysed following isolation using MACS beads (Miltenyi). Total RNA was extracted
414 using Rneasy micro kit (Qiagen) following the manufacturer's instructions. cDNA synthesis was
415 performed using the high capacity cDNA reverse transcriptase kit (Applied Biosystems). Real time PCR
416 was performed using 5ng of CDNA, fast SYBR green master mix (Applied Biosystems) and the following
417 primers: GAPDH forward 5'- CCTGCACCACCAACTGCTTA-3'; reverse 5'- GGCCATCCACAGTCTTCTGAG-
418 3', RPLP0 forward: 5'-GCAATGTTGCCAGTGTCTG-3'; reverse 5'-GCCTTGACCTTTTCAGCAA-3', and
419 ARIDB5 forward 5'-CTGAGCCTCTCCCAGCAGCA-3'; reverse 5'-CGCCTCCTCTGCCACCTTCT-3' on a 7500
420 fast real-time PCR system (Applied Biosystem). GAPDH and RPLP0 were used as housekeeping genes
421 for normalisation. Data were analysed using ΔCt method relative to housekeeping genes and for both
422 control and HIV-1 infected subjects and expressed as log2 expression value.
423
424 **Statistics**
425 Prism 8 (GraphPad Software) and OriginPro 9.1 (OriginLab) were used for statistical analysis as follows:
426 the Mann–Whitney U-test or Student's t-test were used for single comparisons of independent
427 groups, the Wilcoxon-test or Student's paired t-test were used to compare two paired groups. The
428 non-parametric Spearman test was used for correlation analysis. To analyse the confocal imaging
429 results, samples were tested for normality with a Kolmogorov–Smirnov test. The statistical
430 significance for multiple comparisons was assessed with one-way analysis of variance (ANOVA) with
431 Tukey's post hoc test (*$p < 0.05$, **$p < 0.01$, ***$p < 0.001$, and ****$p < 0.0001$).

448
449
450
451

9

References

454 Ahmad, T., K. Aggarwal, B. Pattnaik, S. Mukherjee, T. Sethi, B.K. Tiwari, M. Kumar, A. Micheal, U.
455   Mabalirajan, B. Ghosh, S. Sinha Roy, and A. Agrawal. 2013. Computational classification of
456   mitochondrial shapes reflects stress and redox state. *Cell Death Dis* 4:e461.
457 Altfeld, M., L. Fadda, D. Frleta, and N. Bhardwaj. 2011. DCs and NK cells: critical effectors in the
458   immune response to HIV-1. *Nature reviews. Immunology* 11:176-186.
459 Angin, M., S. Volant, C. Passaes, C. Lecuroux, V. Monceaux, M. Dillies, J. Valle-Casuso, G. Pancino, B.
460   Vaslin, R. Le Grand, L. Weiss, C. Goujard, L. Meyer, F. Boufassa, M. Muller-Trutwin, O.
461   Lambotte, A. Saez-Cirion. 2019. Metabolic plasticity of HIV-specific CD8 T cells is associated
462   with enhanced antiviral potential and natural control of HIV-1 infection. *Nature Metabolism*
463   1:704-716.
464 Bengsch, B., A.L. Johnson, M. Kurachi, P.M. Odorizzi, K.E. Pauken, J. Attanasio, E. Stelekati, L.M.
465   McLane, M.A. Paley, G.M. Delgoffe, and E.J. Wherry. 2016. Bioenergetic Insufficiencies Due to
466   Metabolic Alterations Regulated by the Inhibitory Receptor PD-1 Are an Early Driver of CD8(+)
467   T Cell Exhaustion. *Immunity* 45:358-373.
468 Bradley, T., D. Peppa, I. Pedroza-Pacheco, D. Li, D.W. Cain, R. Henao, V. Venkat, B. Hora, Y. Chen, N.A.
469   Vandergrift, R.G. Overman, R.W. Edwards, C.W. Woods, G.D. Tomaras, G. Ferrari, G.S.
470   Ginsburg, M. Connors, M.S. Cohen, M.A. Moody, P. Borrow, and B.F. Haynes. 2018. RAB11FIP5
471   Expression and Altered Natural Killer Cell Function Are Associated with Induction of HIV
472   Broadly Neutralizing Antibody Responses. *Cell* 175:387-399 e317.
473 Brunetta, E., M. Fogli, S. Varchetta, L. Bozzo, K.L. Hudspeth, E. Marcenaro, A. Moretta, and D. Mavilio.
474   2010. Chronic HIV-1 viremia reverses NKG2A/NKG2C ratio on natural killer cells in patients
475   with human cytomegalovirus co-infection. *AIDS* 24:27-34.
476 Buck, M.D., D. O'Sullivan, R.I. Klein Geltink, J.D. Curtis, C.H. Chang, D.E. Sanin, J. Qiu, O. Kretz, D. Braas,
477   G.J. van der Windt, Q. Chen, S.C. Huang, C.M. O'Neill, B.T. Edelson, E.J. Pearce, H. Sesaki, T.B.
478   Huber, A.S. Rambold, and E.L. Pearce. 2016. Mitochondrial Dynamics Controls T Cell Fate
479   through Metabolic Programming. *Cell* 166:63-76.
480 Chan, D.C. 2019. Mitochondrial Dynamics and Its Involvement in Disease. *Annu Rev Pathol*
481 Chang, C.H., J.D. Curtis, L.B. Maggi, Jr., B. Faubert, A.V. Villarino, D. O'Sullivan, S.C. Huang, G.J. van der
482   Windt, J. Blagih, J. Qiu, J.D. Weber, E.J. Pearce, R.G. Jones, and E.L. Pearce. 2013.
483   Posttranscriptional control of T cell effector function by aerobic glycolysis. *Cell* 153:1239-
484   1251.
485 Cichocki, F., C.Y. Wu, B. Zhang, M. Felices, B. Tesi, K. Tuininga, P. Dougherty, E. Taras, P. Hinderlie, B.R.
486   Blazar, Y.T. Bryceson, and J.S. Miller. 2018. ARID5B regulates metabolic programming in
487   human adaptive NK cells. *The Journal of experimental medicine* 215:2379-2395.
488 Cogliati, S., J.A. Enriquez, and L. Scorrano. 2016. Mitochondrial Cristae: Where Beauty Meets
489   Functionality. *Trends Biochem Sci* 41:261-273.
490 Cong, J., X. Wang, X. Zheng, D. Wang, B. Fu, R. Sun, Z. Tian, and H. Wei. 2018. Dysfunction of Natural
491   Killer Cells by FBP1-Induced Inhibition of Glycolysis during Lung Cancer Progression. *Cell*
492   *Metab* 28:243-255 e245.
493 Cooper, M.A., J.E. Bush, T.A. Fehniger, J.B. VanDeusen, R.E. Waite, Y. Liu, H.L. Aguila, and M.A. Caligiuri.
494   2002. In vivo evidence for a dependence on interleukin 15 for survival of natural killer cells.
495   *Blood* 100:3633-3638.
496 Donnelly, R.P., R.M. Loftus, S.E. Keating, K.T. Liou, C.A. Biron, C.M. Gardiner, and D.K. Finlay. 2014.
497   mTORC1-dependent metabolic reprogramming is a prerequisite for NK cell effector function.
498   *J Immunol* 193:4477-4484.
499 Fauci, A.S., D. Mavilio, and S. Kottilil. 2005. NK cells in HIV infection: paradigm for protection or targets
500   for ambush. *Nature reviews. Immunology* 5:835-843.
501 Fisicaro, P., V. Barili, B. Montanini, G. Acerbi, M. Ferracin, F. Guerrieri, D. Salerno, C. Boni, M. Massari,
502   M.C. Cavallo, G. Grossi, T. Giuberti, P. Lampertico, G. Missale, M. Levrero, S. Ottonello, and C.

503   Ferrari. 2017. Targeting mitochondrial dysfunction can restore antiviral activity of exhausted
504   HBV-specific CD8 T cells in chronic hepatitis B. *Nature medicine* 23:327-336.

505 Garrido, C., M. Abad-Fernandez, M. Tuyishime, J.J. Pollara, G. Ferrari, N. Soriano-Sarabia, and D.M.
506   Margolis. 2018. Interleukin-15-Stimulated Natural Killer Cells Clear HIV-1-Infected Cells
507   following Latency Reversal Ex Vivo. *Journal of virology* 92:

508 Guma, M., M. Budt, A. Saez, T. Brckalo, H. Hengel, A. Angulo, and M. Lopez-Botet. 2006. Expansion of
509   CD94/NKG2C+ NK cells in response to human cytomegalovirus-infected fibroblasts. *Blood*
510   107:3624-3631.

511 Hammer, Q., and C. Romagnani. 2017. OMIP-039: Detection and analysis of human adaptive NKG2C(+)
512   natural killer cells. *Cytometry. Part A : the journal of the International Society for Analytical*
513   *Cytology* 91:997-1000.

514 Hammer, Q., T. Ruckert, E.M. Borst, J. Dunst, A. Haubner, P. Durek, F. Heinrich, G. Gasparoni, M. Babic,
515   A. Tomic, G. Pietra, M. Nienen, I.W. Blau, J. Hofmann, I.K. Na, I. Prinz, C. Koenecke, P. Hemmati,
516   N. Babel, R. Arnold, J. Walter, K. Thurley, M.F. Mashreghi, M. Messerle, and C. Romagnani.
517   2018. Peptide-specific recognition of human cytomegalovirus strains controls adaptive natural
518   killer cells. *Nature immunology* 19:453-463.

519 Keating, S.E., V. Zaiatz-Bittencourt, R.M. Loftus, C. Keane, K. Brennan, D.K. Finlay, and C.M. Gardiner.
520   2016. Metabolic Reprogramming Supports IFN-gamma Production by CD56bright NK Cells. *J*
521   *Immunol* 196:2552-2560.

522 Keppel, M.P., N. Saucier, A.Y. Mah, T.P. Vogel, and M.A. Cooper. 2015. Activation-specific metabolic
523   requirements for NK Cell IFN-gamma production. *J Immunol* 194:1954-1962.

524 Klein Geltink, R.I., D. O'Sullivan, M. Corrado, A. Bremser, M.D. Buck, J.M. Buescher, E. Firat, X. Zhu, G.
525   Niedermann, G. Caputa, B. Kelly, U. Warthorst, A. Rensing-Ehl, R.L. Kyle, L. Vandersarren, J.D.
526   Curtis, A.E. Patterson, S. Lawless, K. Grzes, J. Qiu, D.E. Sanin, O. Kretz, T.B. Huber, S. Janssens,
527   B.N. Lambrecht, A.S. Rambold, E.J. Pearce, and E.L. Pearce. 2017. Mitochondrial Priming by
528   CD28. *Cell* 171:385-397 e311.

529 Lee, J., T. Zhang, I. Hwang, A. Kim, L. Nitschke, M. Kim, J.M. Scott, Y. Kamimura, L.L. Lanier, and S. Kim.
530   2015. Epigenetic modification and antibody-dependent expansion of memory-like NK cells in
531   human cytomegalovirus-infected individuals. *Immunity* 42:431-442.

532 Llufrio, E.M., L. Wang, F.J. Naser, and G.J. Patti. 2018. Sorting cells alters their redox state and cellular
533   metabolome. *Redox Biol* 16:381-387.

534 Marcais, A., J. Cherfils-Vicini, C. Viant, S. Degouve, S. Viel, A. Fenis, J. Rabilloud, K. Mayol, A. Tavares,
535   J. Bienvenu, Y.G. Gangloff, E. Gilson, E. Vivier, and T. Walzer. 2014. The metabolic checkpoint
536   kinase mTOR is essential for IL-15 signaling during the development and activation of NK cells.
537   *Nature immunology* 15:749-757.

538 Martin, M.P., X. Gao, J.H. Lee, G.W. Nelson, R. Detels, J.J. Goedert, S. Buchbinder, K. Hoots, D. Vlahov,
539   J. Trowsdale, M. Wilson, S.J. O'Brien, and M. Carrington. 2002. Epistatic interaction between
540   KIR3DS1 and HLA-B delays the progression to AIDS. *Nature genetics* 31:429-434.

541 Martin, M.P., Y. Qi, X. Gao, E. Yamada, J.N. Martin, F. Pereyra, S. Colombo, E.E. Brown, W.L. Shupert,
542   J. Phair, J.J. Goedert, S. Buchbinder, G.D. Kirk, A. Telenti, M. Connors, S.J. O'Brien, B.D. Walker,
543   P. Parham, S.G. Deeks, D.W. McVicar, and M. Carrington. 2007. Innate partnership of HLA-B
544   and KIR3DL1 subtypes against HIV-1. *Nature genetics* 39:733-740.

545 Mela, C.M., and M.R. Goodier. 2007. The contribution of cytomegalovirus to changes in NK cell
546   receptor expression in HIV-1-infected individuals. *The Journal of infectious diseases* 195:158-
547   159; author reply 159-160.

548 Merino, A., B. Zhang, P. Dougherty, X. Luo, J. Wang, B.R. Blazar, J.S. Miller, and F. Cichocki. 2019.
549   Chronic stimulation drives human NK cell dysfunction and epigenetic reprograming. *The*
550   *Journal of clinical investigation* 130:3770-3785.

551 Michelet, X., L. Dyck, A. Hogan, R.M. Loftus, D. Duquette, K. Wei, S. Beyaz, A. Tavakkoli, C. Foley, R.
552   Donnelly, C. O'Farrelly, M. Raverdeau, A. Vernon, W. Pettee, D. O'Shea, B.S. Nikolajczyk, K.H.G.

11

553   Mills, M.B. Brenner, D. Finlay, and L. Lynch. 2018. Metabolic reprogramming of natural killer
554   cells in obesity limits antitumor responses. *Nature immunology* 19:1330-1340.
555   Miyazono, Y., S. Hirashima, N. Ishihara, J. Kusukawa, K.I. Nakamura, and K. Ohta. 2018. Uncoupled
556   mitochondria quickly shorten along their long axis to form indented spheroids, instead of
557   rings, in a fission-independent manner. *Scientific reports* 8:350.
558   O'Brien, K.L., and D.K. Finlay. 2019. Immunometabolism and natural killer cell responses. *Nature*
559   *reviews. Immunology* 19:282-290.
560   O'Sullivan, T.E., L.R. Johnson, H.H. Kang, and J.C. Sun. 2015. BNIP3- and BNIP3L-Mediated Mitophagy
561   Promotes the Generation of Natural Killer Cell Memory. *Immunity* 43:331-342.
562   Peppa, D., I. Pedroza-Pacheco, P. Pellegrino, I. Williams, M.K. Maini, and P. Borrow. 2018. Adaptive
563   Reconfiguration of Natural Killer Cells in HIV-1 Infection. *Frontiers in immunology* 9:474.
564   Pfeifer, C., A.J. Highton, S. Peine, J. Sauter, A.H. Schmidt, M.J. Bunders, M. Altfeld, and C. Korner. 2018.
565   Natural Killer Cell Education Is Associated With a Distinct Glycolytic Profile. *Frontiers in*
566   *immunology* 9:3020.
567   Previte, D.M., C.P. Martins, E.C. O'Connor, M.L. Marre, G.M. Coudriet, N.W. Beck, A.V. Menk, R.H.
568   Wright, H.M. Tse, G.M. Delgoffe, and J.D. Piganelli. 2019. Lymphocyte Activation Gene-3
569   Maintains Mitochondrial and Metabolic Quiescence in Naive CD4(+) T Cells. *Cell reports*
570   27:129-141 e124.
571   Rolle, A., M. Meyer, S. Calderazzo, D. Jager, and F. Momburg. 2018. Distinct HLA-E Peptide Complexes
572   Modify Antibody-Driven Effector Functions of Adaptive NK Cells. *Cell reports* 24:1967-1976
573   e1964.
574   Schafer, J.R., T.C. Salzillo, N. Chakravarti, M.N. Kararoudi, P. Trikha, J.A. Foltz, R. Wang, S. Li, and D.A.
575   Lee. 2019. Education-dependent activation of glycolysis promotes the cytolytic potency of
576   licensed human natural killer cells. *The Journal of allergy and clinical immunology* 143:346-
577   358 e346.
578   Schlums, H., F. Cichocki, B. Tesi, J. Theorell, V. Beziat, T.D. Holmes, H. Han, S.C. Chiang, B. Foley, K.
579   Mattsson, S. Larsson, M. Schaffer, K.J. Malmberg, H.G. Ljunggren, J.S. Miller, and Y.T.
580   Bryceson. 2015. Cytomegalovirus infection drives adaptive epigenetic diversification of NK
581   cells with altered signaling and effector function. *Immunity* 42:443-456.
582   Schurich, A., L.J. Pallett, D. Jajbhay, J. Wijngaarden, I. Otano, U.S. Gill, N. Hansi, P.T. Kennedy, E.
583   Nastouli, R. Gilson, C. Frezza, S.M. Henson, and M.K. Maini. 2016. Distinct Metabolic
584   Requirements of Exhausted and Functional Virus-Specific CD8 T Cells in the Same Host. *Cell*
585   *reports* 16:1243-1252.
586   Scully, E., and G. Alter. 2016. NK Cells in HIV Disease. *Current HIV/AIDS reports* 13:85-94.
587   van der Windt, G.J., B. Everts, C.H. Chang, J.D. Curtis, T.C. Freitas, E. Amiel, E.J. Pearce, and E.L. Pearce.
588   2012. Mitochondrial respiratory capacity is a critical regulator of CD8+ T cell memory
589   development. *Immunity* 36:68-78.
590   Webb, G.M., S. Li, G. Mwakalundwa, J.M. Folkvord, J.M. Greene, J.S. Reed, J.J. Stanton, A.W. Legasse,
591   T. Hobbs, L.D. Martin, B.S. Park, J.B. Whitney, E.K. Jeng, H.C. Wong, D.F. Nixon, R.B. Jones, E.
592   Connick, P.J. Skinner, and J.B. Sacha. 2018. The human IL-15 superagonist ALT-803 directs SIV-
593   specific CD8(+) T cells into B-cell follicles. *Blood Adv* 2:76-84.
594   Zhang, T., J.M. Scott, I. Hwang, and S. Kim. 2013. Cutting edge: antibody-dependent memory-like NK
595   cells distinguished by FcRgamma deficiency. *J Immunol* 190:1402-1406.
596
597
598   **Figure Legends**
599   **Fig. 1. Analysis of the basal metabolic profile of NK cell in control (CTR) and HIV-1 infected donors.**
600   **(A)** Real-time analysis of aerobic glycolysis (ECAR) in purified NK cells **(B)** Basal ECAR, **(C)** maximal
601   ECAR, **(D)** glycolysis and (**E**) glycolytic reserve in isolated NK cells from n=6 controls (CTR) and n=8
602   chronic HIV-1 patients (HIV-1). **(F)** Real-time analysis of oxygen consumption rate (OCR) in isolated NK
603   cells from both groups of study. (**G**) Basal OCR, **(H)** maximal OCR (OCR max) and **(I)** Spare respiratory
604   capacity (SRC). Bars show mean ± SEM. Correlation between maximal OCR and **(J)** *ex vivo* percentage

12

605 of adaptive CD57+NKG2C+ CD56dim NK cells and **(K)** proportion of CD57+NKG2C+CD56dimIFN-γ_+ after
606 CD16 triggering. The non-parametric Spearman test was used for correlation analysis. Sample
607 triplicates were used for Seahorse assays. Significance determined by Mann-Whitney *U* test, ns: non-
608 significant, *p<0.05, **p<0.01
609
610 **Fig. 2. Metabolic requirements of NK cells for IFN-γ production after CD16 activation.**
611 **(A)** Representative flow plots and summary data of fold change in IFN-γ production by CD56dim NK
612 cells following anti-CD16 plate bound stimulation from **(B)** n=6 healthy controls (CTR) and **(C)** n=7
613 chronic HIV-1 infected patients (HIV-1) in the presence or absence of the different metabolic
614 inhibitors: Oligomycin (100 nM), 2-DG (50 mM), UK5099 (2 μM), BPTES (3 μM) or Etomoxir (4 μM).
615 Fold change was normalised to anti-CD16 stimulation alone (set to 1 and indicated as a dotted line).
616 Bars show mean ± SD and each symbol represents data from an individual donor. Wilcoxon matched-
617 pairs signed rank test,*p<0.05.
618
619 **Fig. 3. Evaluation of NK cell mitochondrial health. (A)** Representative flow plots and (**B**) box and
620 whisker plots depicting the ratio of polarised over depolarised mitochondrial (mitochondrial
621 membrane potential (ΔΨm), of total CD56dim NK cells and NK cell subsets by JC-1 staining in control
622 (CTR) and HIV-1 infected subjects (HIV-1). JC-1 red staining designates polarised mitochondria, while
623 loss of JC-1 red shows depolarisation. The box-and-whisker plots show the median, quartiles, and
624 range. Data from an individual subject are represented by each symbol. Significance determined by
625 Mann-Whitney *U* test. **(C)** Representative confocal images of mitochondria (red) from purified NK cells
626 from a control and an HIV-1 infected donor. The NK cell membrane was visualised by staining with
627 wheat germ agglutinin (green). **(D)** Quantification of mitochondria numbers, **(E)** area, **(F)** sphericity
628 and (**G**) volume in purified NK cells from both n=3 controls (CTR) and n=3 HIV-1 seropositive donors
629 (HIV-1). Each symbol represents the mean value from one cell. Data are from a minimum of 50 cells
630 from three independent donors. Bars represent mean ± SD. ns: non-significant, **p<0.01, ***p<0.001,
631 ****p<0.0001, one-way analysis of variance (ANOVA) with Tukey's post-hoc test.
632
633 **Fig. 4. IL-15 treatment ameliorates NK cell metabolic requirements for receptor stimulation in HIV-
634 1 infection. (A)** Representative flow plots and (**B**) summary data of fold change in IFN-γ production by
635 CD56dim NK cells following stimulation with anti-CD16 with or without IL-15 pre-treatment and in the
636 presence or absence of the following inhibitors: Oligomycin (100 nM) or 2-DG (50 mM), from n=5 HIV-
637 1 infected donors. Data normalised to anti-CD16 stimulation alone, set to 1 and indicated as a dotted
638 line in the graph. Bars mean ± SD and each symbol indicates individual responses. **(C)** Representative
639 histograms and **(D)** summary bar charts of pS6 expression levels to evaluate mTORC1 activity after
640 stimulation in CD56dim NK cells from n=5 HIV-1 infected individuals. Statistics by Wilcoxon matched-
641 pairs test. (**E**) Real-time analysis of aerobic glycolysis (ECAR), **(F)** oxygen consumption (OCR) and **(G)**
642 basal OCR:ECAR ratio in purified NK cells from n=3 HIV-1 donors in the presence or absence of anti-
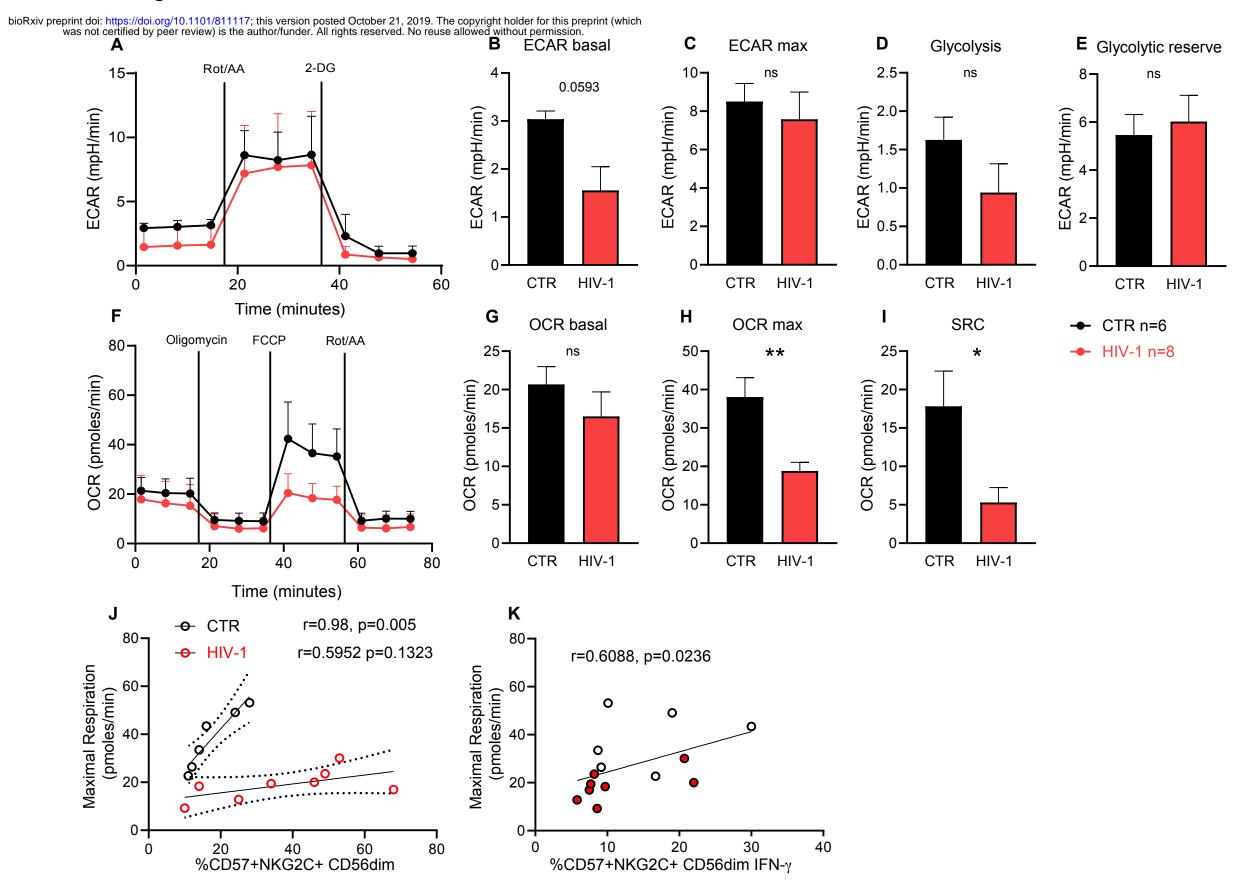643 CD16 and/or IL-15 pre-treatment. *p<0.05 by paired Student's *t*-test.
644
645
646 **Supplementary material**
647 **Fig. S1. Gating strategy to distinguish canonical and adaptive NK cells. (A)** Representative example
648 gated on live CD3-, CD14-, CD19- lymphocytes; CD56 and CD16 are used to identify natural killer (NK)
649 cell subsets. **(B)** Representative examples from a healthy control and an HIV-1 infected patient
650 showing frequencies of canonical NK cells defined as CD56dimCD57+NKG2C- and adaptive NK cells
651 defined as CD56dimCD57+NKG2C+.
652
653 **Fig. S2. Metabolic requirements of different NK cell subsets for IFN-γ production after CD16
654 activation.** Representative flow plots of CD57+NKG2C- CD56dim (canonical) **(A)** and CD57+NKG2C+
655 CD56dim (adaptive) NK cells from a control (CTR) and an HIV-1 infected donor (HIV-1) **(D)** showing

13

IFN-γ production following anti-CD16 stimulation in the absence and presence of the indicated metabolic inhibitors. Summary bar charts of fold change in IFN-γ production by canonical NK cells following anti-CD16 plate bound stimulation from **(B)** n=6 control individuals and **(C)** n=7 HIV-1 infected donors and by adaptive NK cells from **(E)** n=6 control individuals and **(F)** n=7 HIV-1 infected subjects in the presence or absence of the different metabolic inhibitors: Oligomycin (100 nM), 2-DG (50 mM), UK5099 (2 μM), BPTES (3 μM) or Etomoxir (4 μM). Fold change was normalised to anti-CD16 stimulation alone (set to 1 and indicated as a dotted line). Bars show mean ± SD and each symbol represents data from an individual donor. Wilcoxon matched-pairs signed rank test *p<0.05

Movie S3. Representative confocal z-stack, 3D projection and reconstruction of mitochondrial distribution in a primary human NK cell isolated from a CMV+ control. Mitochondria, red; cell membrane, green.

Movie S4: Representative confocal z-stack, 3D projection and reconstruction of mitochondrial distribution in a primary human NK cell isolated from an HIV-1 infected donor. Mitochondria, red; cell membrane, green.

Fig. S5. Quantification of gene expression by RT-qPCR for **(A)** *ARID5B* in isolated NK cells from n=4 HCMV+ control donors and n=4 HIV-1 infected subjects. All relative expression values were calculated by normalising against GAPDH as a housekeeping gene. **p<0.01

Fig. S6. IL-15 treatment ameliorates NK cell subsets metabolic requirements for receptor stimulation in HIV-1 infection. Representative flow plots **(A, B)** and summary bar charts of fold change in IFN-γ production by **(C)** canonical and **(D)** adaptive NK cells following stimulation with anti-CD16 with or without IL-15 pre-treatment and in the presence or absence of the following inhibitors: Oligomycin (100 nM) or 2-DG (50 mM), from n=5 HIV-1 infected donors. Fold change was normalised to anti-CD16 stimulation alone (set to 1 and indicated as a dotted line). Bars show mean ± SD and each symbol represents data from an individual donor. Statistics by Wilcoxon matched-pairs test.
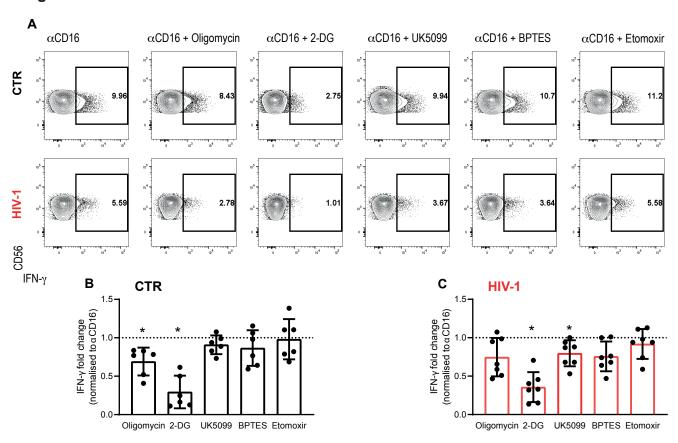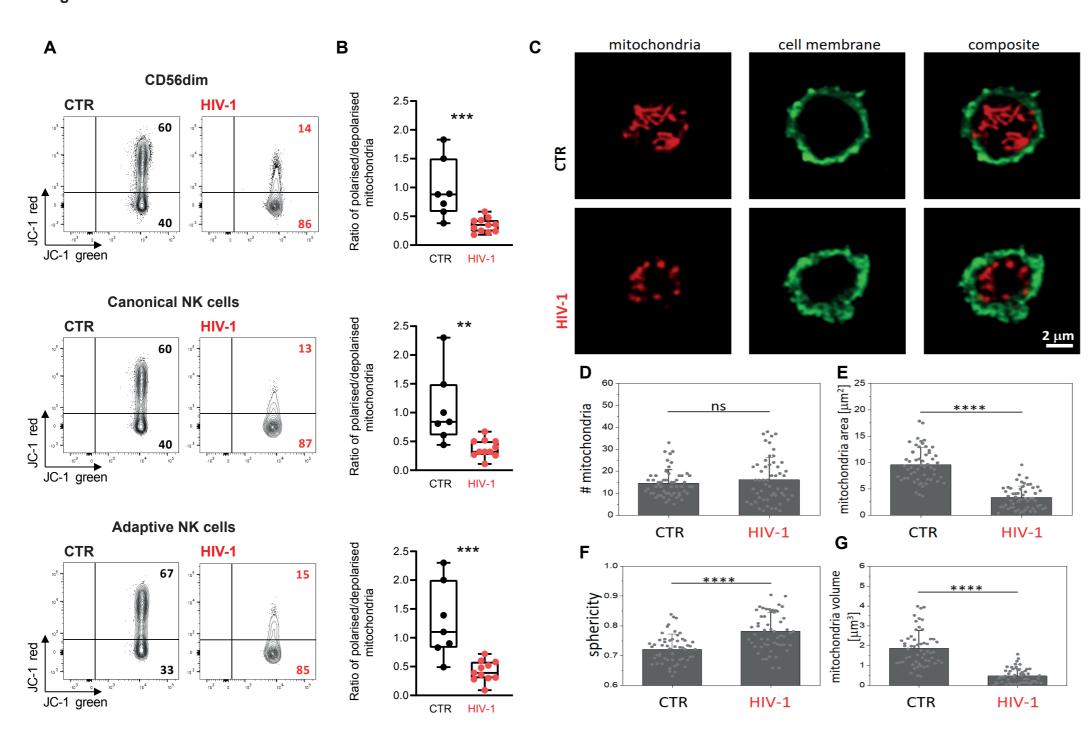
Fig. 1

Fig. 2

Fig. 3

Fig. 4

A

αCD16 αCD16 + Oligomycin αCD16 + 2-DG

Untreated

5.45 2.76 0.89

IL-15 pre-treatment

52.5 68.1 51.9

CD56

IFN-γ

B

+ Oligomycin

IFN-γ fold change (normalised to αCD16)

αCD16   +   +
IL-15 pre-treatment   −   +

+ 2-DG

IFN-γ fold change (normalised to αCD16)

αCD16   +   +
IL-15 pre-treatment   −   +

C

% of Max

Basal gMFI: 399
αCD16 gMFI: 384
IL-15 pre-treatment +αCD16 gMFI: 714

pS6

D

pS6 gMFI

0.0625

αCD16   −   +   +
IL-15 pre-treatment   −   −   +

E

ECAR (mpH/min)

Rot/AA   2-DG

Time (minutes)

F

OCR (pmoles/min)

Oligomycin   FCCP   Rot/AA

Time (minutes)

Basal
IL-15 pre-treatment
IL-15 pre-treatment +αCD16

G

OCR:ECAR

*

0.0617

αCD16   −   −   +
IL-15 pre-treatment   −   −   +